

INFLUENCE OF BACKFILLED SAND DIMENSIONS AND LOCATION ON SHAFT RESISTANCE OF PILES

Kenta Nakamura¹ and *Hiroshi Nagai²

¹ Division of Sustainable and Environmental Engineering, Graduate School of Engineering, Muroran Institute of Technology, Japan

² College of Design and Manufacturing Technology, Muroran Institute of Technology, Japan

*Corresponding Author, Received: 24 July 2023, Revised: 2 Aug. 2023, Accepted: 7 Aug. 2023

ABSTRACT: In this study, compressive loading tests of pile-overlapping backfilled soil were performed to investigate the effect of the dimensions and location of backfilled sand with different densities on the shaft resistance of the pile. The results showed that when the backfilled soil is dense sand, the shaft resistance is affected by the dimensions and location of the sand. The earth pressure at which the maximum value of the shaft resistance is reached is shown to be related to the distance from the outer surface of the pile to the outer edge of the backfilled sand (i.e., the width of the backfilled sand). Thereafter, a method was developed to evaluate the earth pressure related to the shaft resistance of the pile according to the width of the backfilled sand by dividing the sand into several segments in the circumferential direction. Based on these results, a calculation method was developed to calculate the maximum axial resistance of the pile considering various conditions (dimensions, location, and density) of the backfilled sand.

Keywords: Pile shaft resistance, Backfilled soil, Dilatancy, Earth pressure, Loading test

1. INTRODUCTION

Often, existing old pile foundations need to be dismantled and removed along with other underground obstructions during the demolition of a building. When old pile foundations are removed, their holes should, in principle, be backfilled to match the conditions of the surrounding ground. However, backfilled soil has often been noted to exhibit heterogeneity with the surrounding ground. Therefore, when new piles are inserted close to the backfilled soil after the removal of existing piles, the load-bearing performance of the new piles may be affected.

Many previous studies focused on the shaft resistance of piles. For example, centrifuge model loading tests have been conducted to investigate the pile shaft capacity in sandy soil [1,2]. In these tests, changes in the horizontal stress acting on the pile shaft were measured. The measured stress changes were found to be determined by the radial stiffness of the sand mass and the dilation of the shear band at the pile-sand interface. Finite element analyses using a two-surface plasticity constitutive model were performed to examine the changes in the stress state around the shaft upon axial loading of the pile [3,4]. An analytical approach to estimate the shaft capacity of piles bored in sandy soils was presented. This approach is based on explicitly modeling the shear band and on the fundamental mechanical behavior of sandy soil [5]. An elasto-plastic model based on critical state soil mechanics and

generalized plasticity was used to simulate the monotonic and cyclic 3D behavior of soil-structure interfaces [6]. An interface constitutive model in conjunction with a pile segment analysis was proposed to predict the shaft resistance achieved by non-displacement piles [7,8]. Digital images of the model pile and sand were taken during loading tests in a half-cylindrical calibration chamber to obtain the soil displacement and strain fields [9]. A simple shear test with an imposed constant normal stiffness was carried out to investigate the mechanical behavior at the sand-pile interface [10]. Direct shear tests under a large number of loading cycles were conducted to reveal the effects of cyclic shear amplitudes and loading sequences on a soil-structure interface [11]. Furthermore, simulations of loading tests using 3D finite element analyses were also performed [12]. The results showed that the mobilized lateral earth pressure coefficient along the pile shaft increases with increasing relative density and decreasing initial confining stress. The frictional characteristics of the soil-structure interface and the associated displacement localization under constant normal stiffness conditions are investigated at both macroscales and microscales by using the discrete element method (DEM) [13]. In contrast, the present study focuses on the shaft resistance of piles with overlapping backfilled soil after the removal of existing piles. A previous study simulated the backfilling process for soil and conducted compressive loading tests on piles installed near backfilled sand columns [14].

Simulations of loading tests using the finite element method were also performed. The results showed that if the conditions for the backfilled sand are different from those for the surrounding soil, the maximum shaft resistance of the pile differs depending on the density of the backfilled sand column. Furthermore, the analysis indicated that the backfilled sand changed the shape and thickness of the shear band near the pile. Therefore, compressive loading tests were performed to quantify the shear failure behavior of the soil adjacent to the pile [15]. In these tests, several layers of colored sand were placed in the model soil to visualize the location of shear failure. However, the dimensions and location of existing old piles generally depend on the building conditions.

In this study, compressive loading tests of a pile with different dimensions and locations of the backfilled soil were conducted to investigate the effect of each parameter (dimensions, location, and density) for the backfilled soil, especially on the shaft resistance of the piles and the earth pressure near the pile that contributes to the shaft resistance. As a result, it was confirmed that the earth pressure near the pile varied greatly depending on the condition of the backfilled soil; the calculation method presented in the previous study could not adequately evaluate the shaft resistance. Therefore, a new method for evaluating the horizontal earth pressure focusing on the relationship between the change in horizontal earth pressure and the dimensions and location of the backfilled soil was investigated. Based on the investigation, a calculation method for the shaft resistance for piles that consider backfilled soil was developed.

2. RESEARCH SIGNIFICANCE

It is important in the design of pile foundations to reveal the bearing capacity of new piles overlapped by backfilled soil because the conditions of the soil backfilled after the removal of existing piles often differ from those of the surrounding soil. As the existing construction stock of high-rise buildings is being rebuilt and larger foundation piles are removed, the results of this research are very significant in designing foundations that properly account for the uncertainties in the ground.

3. AXIAL COMPRESSIVE LOADING TEST OF PILE-OVERLAPPING BACKFILLED SOIL

Fig.1 shows an overview of the experimental equipment for the loading test. The model soil used to build the specimen was dry Tohoku quartz sand number 6 (maximum density 1.71 g/cm³, minimum density 1.40 g/cm³, mean grain size 0.3 mm).

The soil was prepared at an arbitrary relative density ($D_r = 60\%$) using air pluviation in a cylindrical chamber. After 300 mm of sand was deposited in the chamber, a model pile was set up in the center of the chamber. The tip of the pile was inserted into a cylindrical jig to eliminate the tip resistance. To simulate the case where the new pile overlaps the backfilled soil after an existing pile was removed, a crescent-shaped casing made from a 0.3-mm-thick copper plate was placed close to the pile. The casing was filled with sand at an arbitrary relative density, and the casing was pulled out after it was full. During the preparation of the soil and backfilled sand, colored 2-mm-thick sand layers were laid at 50-mm intervals. The colored sand layers were placed to confirm the shear failure location after the loading test. The model soil was finally added to a height of 600 mm.

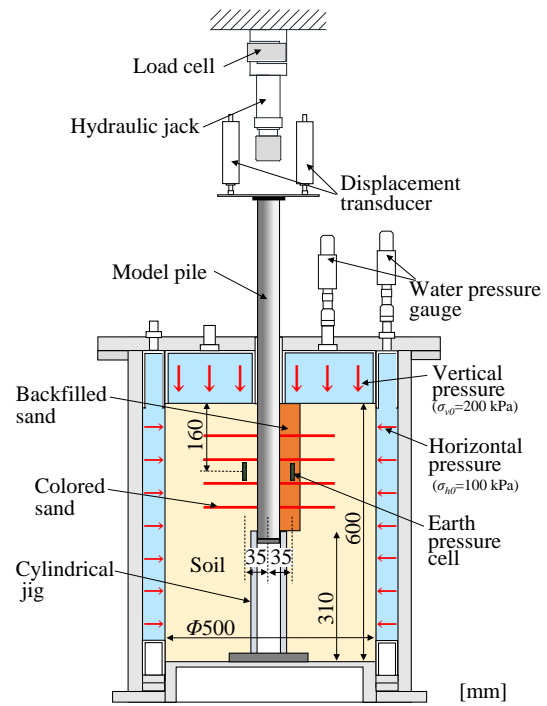


Fig.1 Outline of the experimental equipment

The model pile, shown in Fig.2, was an aluminum pipe with a diameter, d , of 30 mm and a thickness of 2 mm. A thermal spray coating was applied to the surface of the pile shaft in order to roughen it and increase the shaft resistance like a cast-in-place pile. Strain gauges were attached inside the pile to check the distribution of axial force along the pile. The tip of the pile was capped. This cap prevented the strain gauges from being damaged by sand entering the pile during loading tests or by soil wetting after loading tests. The effective embedded length of the pile on which the shaft resistance acted was 280 mm.

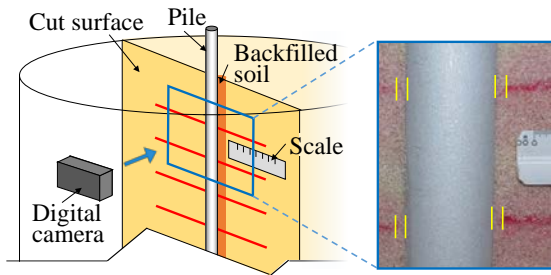


Fig.6 Schematic diagram of observation of shear in colored sand layers

Fig.7 shows the layout of the pile and backfilled sand. The parameters set in this experiment were the dimensions (d_{bs}), location (R), and relative density (D_r) of the backfilled sand. Two ratios of backfilled sand diameter to pile diameter ($d_{bs}/d = 2.0, 3.0$) and two degrees of overlap of backfilled sand to pile ($R/d = 0.5, 0.75$) were set. Two relative densities of backfilled sand, low density ($D_r = 30\%$) and high density ($D_r = 80\%$), were used in the combined dimensions and location pattern. A total of six pile loading tests were performed, as listed in Table 1.

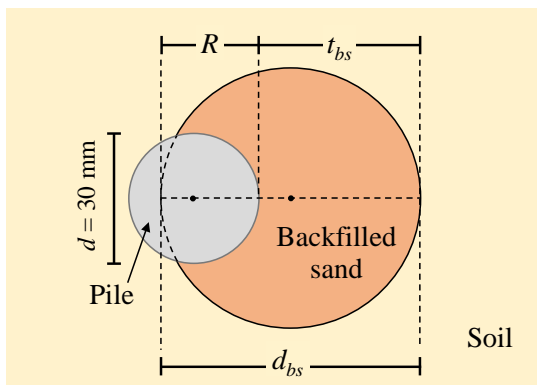


Fig.7 Layout of the pile and backfilled sand

Table 1 Test cases

Model name	L_B2.0-R0.5	D_B2.0-R0.5	L_B2.0-R0.75	D_B2.0-R0.75	L_B3.0-R0.5	D_B3.0-R0.5
Soil	M	M	M	M	M	M
Backfilled sand	L	D	L	D	L	D
d_{bs}/d	2.0	2.0	2.0	2.0	3.0	3.0
R/d	0.5	0.5	0.75	0.75	0.5	0.5

note: L: Loose sand ($D_r = 30\%$), M: Medium sand ($D_r = 60\%$), D: Dense sand ($D_r = 80\%$)

Table 2 Mechanical properties of sand

	L	M	D
Relative density, D_r (%)	30	60	80
Internal friction angle, ϕ (deg.)	29.3	32.1	34.9

note: Cohesion of sand is almost zero.

The mechanical properties of the sand are shown in Table 2. The internal friction angle for the sand was obtained by direct shear tests under constant normal stress conditions.

4. RESULTS AND DISCUSSION

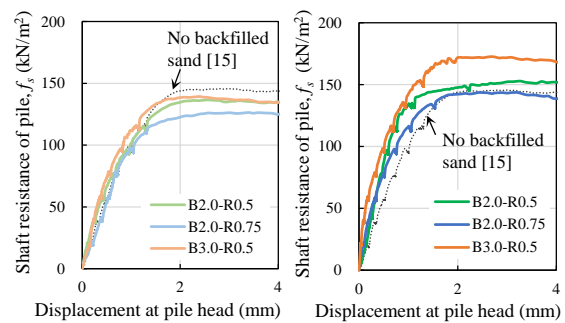
4.1 Shaft Resistance of Pile

Fig.8 shows the relationship between the shaft resistance of the pile and the settlement at the pile head. The shaft resistance of the pile, f_s , was calculated by dividing the axial force difference between the pile head and the pile tip ($G1$ in Fig.2) by the embedded pile shaft area. The shaft resistance of the pile reached a maximum value, f_{smax} , at about 2 mm of settlement, regardless of the dimensions and location of the backfilled sand.

First, we focus on the effect of the backfilled sand dimensions on the maximum pile shaft resistance. A comparison of cases L_B2.0-R0.5 and L_B3.0-R0.5, which used low-density backfilled sand, shows a small difference in f_{smax} between them. Conversely, when the density of the backfilled sand is high, f_{smax} for D_B3.0-R0.5, which has a larger volume of backfilled sand, is 14% larger than that for D_B2.0-R0.5, which has a smaller volume.

Next, we focus on the effect of the degree of overlap of the backfilled sand with the pile on f_{smax} . When the density of the backfilled sand is low, f_{smax} for L_B2.0-R0.75 is 8% smaller than that for L_B2.0-R0.5, and when the density of the backfilled sand is high, f_{smax} for D_B2.0-R0.75 is 6% smaller than that for D_B2.0-R0.5. Regardless of the density of the backfilled sand, the larger the degree of overlap, the smaller the value of f_{smax} .

Therefore, for the loose backfilled sand, f_{smax} depends on the circumferential proportion of the pile in contact with the backfilled sand. For the dense backfilled sand, f_{smax} may depend on the width of the backfilled sand, which is determined by the geometrical configuration of the dimensions and location.



(a) Low density (L) (b) High density (D)

Fig.8 Shaft resistance of the pile versus displacement at the pile head

4.2 Earth Pressure

Fig.9 shows the relationship between the horizontal earth pressure and the settlement at the pile head. The horizontal earth pressure is the average value measured at earth pressure cells A and C, as shown in Fig.3. The horizontal earth pressure tends to increase up to around 2 mm of settlement, where the maximum value of the shaft resistance is observed. In case D_B2.0-R0.5, the horizontal earth pressure is underestimated concerning f_{smax} . This is because the increase in soil pressure was small when the confining pressure was applied to the soil, implying that the soil around the earth pressure cell was disturbed when it was installed.

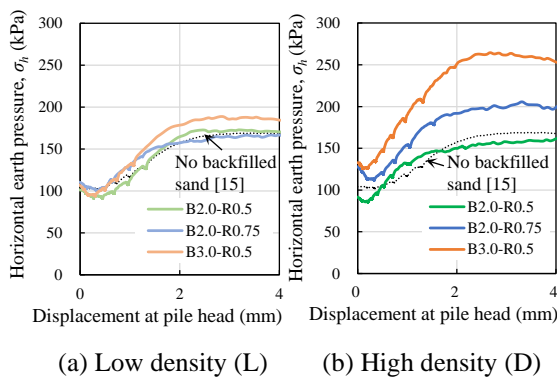


Fig.9 Measured horizontal earth pressure

4.3 Shear Band

Fig.10 shows the average thickness of the shear band measured from the four colored sand layers. The thickness of the shear band, α , ranged from 1.5 to 2.5 mm (5.0 to $7.8D_{50}$) with no clear correlation to the backfilled sand conditions (dimensions, location, and relative density). The results were intermediate between the experimental results of Uesugi et al. [16] ($\alpha = 3$ to $4D_{50}$) and those of Nemat-Nasser et al. [17] ($\alpha = 10$ to $15D_{50}$).

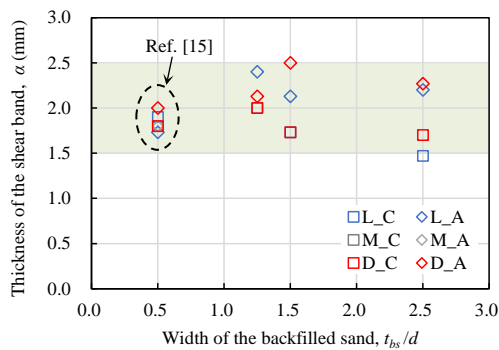


Fig.10 Measured thickness of shear band

5. HORIZONTAL EARTH PRESSURE

Based on experimental results, the relationship between the change in horizontal earth pressure and the dimensions and location of the backfilled soil was investigated. To evaluate the horizontal earth pressure, the soil near the pile was divided into three zones, as shown in Fig.11: the area of backfilled sand (zone A), an equivalent area of earth on the opposite side of the pile (zone C), and other areas (zone B) [15].

The horizontal earth pressure near the pile changes due to the volumetric change caused by shear deformation of the soil near the pile as the pile is pushed down, as shown in Fig.12. Therefore, the horizontal earth pressure is greater closer to the pile.

The horizontal earth pressure acting on the shear failure surface near the pile at the point when the shaft resistance of the pile reaches its maximum value was estimated from the experimentally obtained measurements as explained below.

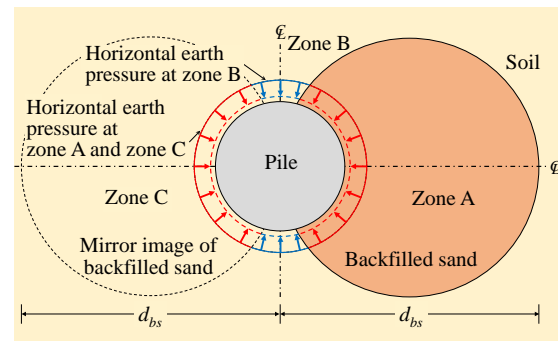


Fig.11 Schematic diagram of earth pressure

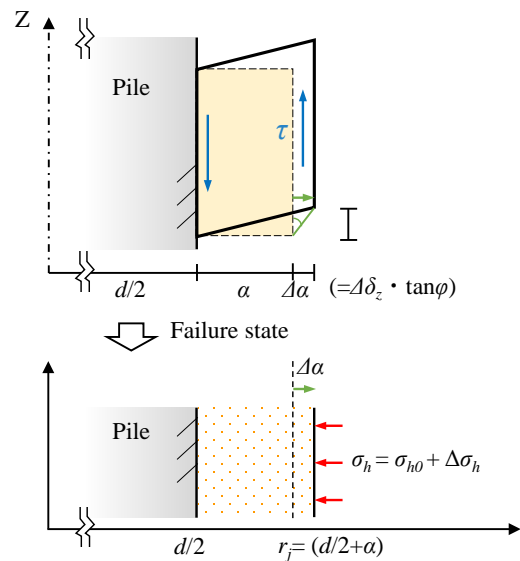


Fig.12 Variation of horizontal earth pressure due to expansion in dilatant soil

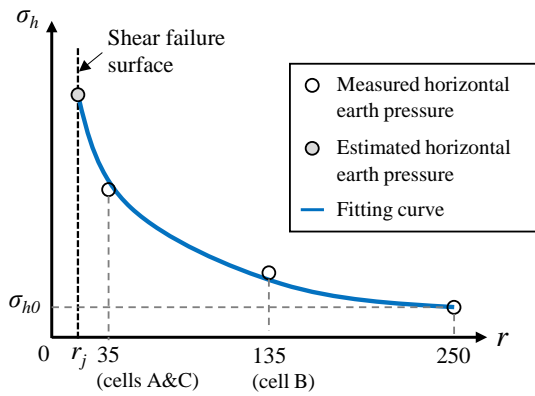


Fig.13 Approximation of the horizontal earth pressure distribution

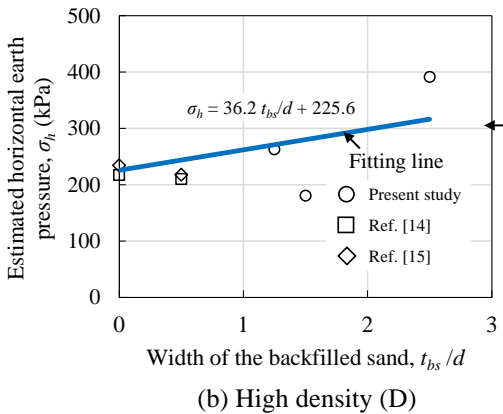
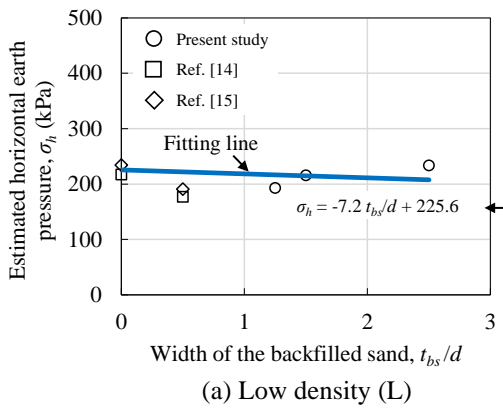


Fig.14 Relationship between the thickness of backfilled sand and estimated horizontal earth pressure at failure surface

In the loading tests, the horizontal earth pressures were measured in the radial direction from the pile axis at $r = 35$ mm (earth pressure cells A and C), $r = 135$ mm (earth pressure cell B), and $r = 250$ mm (confining pressure on the soil). As described above, the soil pressures in zones A and C are balanced, so $r = 35$ mm is evaluated as the

average value obtained from soil pressure cells A and C. The horizontal earth pressure at the shear failure surface was then estimated using an exponential approximation of the earth pressure distribution [18] representing the measurements at the three locations, as shown in Fig.13. The shear failure surface was assumed to be occurring at $r = 17$ mm, with the shear zone thickness assumed to be the average of the measured values, or $\alpha = 2.0$ mm.

Fig.14 shows the relationship between the backfilled sand width and the estimated horizontal earth pressure for each relative density of backfilled soil. The backfilled sand width is expressed as t_{bs}/d , which is normalized by dividing by the pile diameter. For the dense backfilled sand, it was observed that the horizontal earth pressure tended to increase as the backfilled sand width increased. Therefore, the horizontal earth pressure was approximated by a linear function with an intercept on the vertical axis for the condition of the previous experiment [15] without backfilled sand ($t_{bs}/d = 0$). As the width of the backfilled sand increases, the horizontal earth pressure approaches the value (indicated by the left-pointing arrow in Fig.14) for low-density or high-density sand [15], where there is no backfilled sand.

6. METHOD FOR CALCULATING PILE SHAFT RESISTANCE

The width of the backfilled sand, t_{bs} , varies with the circumferential direction of the pile. Therefore, the horizontal earth pressure that contributes to the shaft resistance of the pile was evaluated by dividing the area of backfilled sand into n segments around the circumference of the pile, as shown in Fig.15.

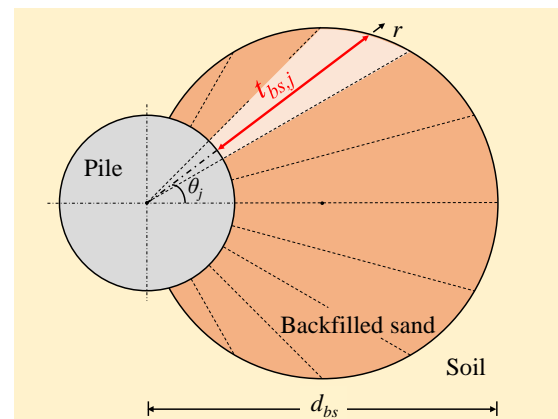


Fig.15 Width of backfilled sand, t_{bs} , after it is divided into n segments

The horizontal earth pressure for the divided backfilled sand, $\sigma_{h,j}$, is evaluated according to the

width, $t_{bs,j}$, of each segment using the approximation formula in Fig.14. The width, $t_{bs,j}$, of each segment can be expressed by Eqs. (1) and (2) using the law of cosines for the triangle shown in Fig.16.

$$t_{bs,j} = \sqrt{(s \cdot \cos\theta_j)^2 - s^2 + \left(\frac{d_{bs}}{2}\right)^2} \quad (1)$$

$$+ s \cdot \cos\theta_j - \frac{d}{2}$$

$$s = \frac{d}{2} + \frac{d_{bs}}{2} - R \quad (2)$$

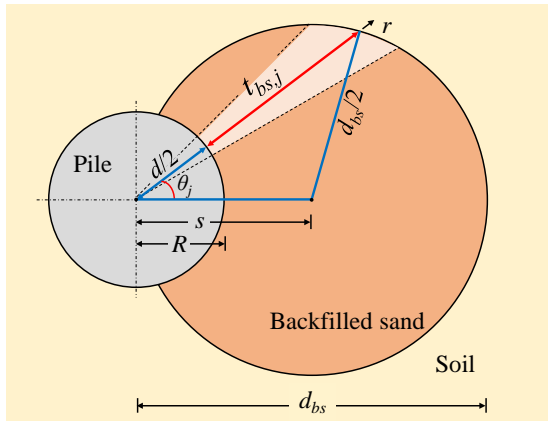


Fig.16 Schematic of pile and backfilled sand width

The shear stress, τ_j , for each element can be expressed by Eqs. (3) and (4) [3] using the horizontal earth pressure, $\sigma_{h,j}$, at the location of shear failure and the internal friction angle, ϕ_j , for the soil (see Table 2), based on the theory of shear failure of the soil.

$$\tau_j = \sigma_{h,j} \cdot \tan\phi_j' \quad (3)$$

$$\phi_j' = \tan^{-1}(\sin\phi_j) \quad (4)$$

The shaft resistance of the pile is the sum of the shear stress, τ_j , for each element multiplied by the ratio η_j [15] to the circumferential length at the shear failure surface. Therefore, the maximum shaft resistance, $f_{s,cal}$, of the pile considering the shear stresses in the three regions from zone A to zone C can be expressed as

$$f_{s,cal} = \frac{d + 2\alpha}{d} \left\{ \sum_{i=1}^n (\tau_{a,i} \cdot \eta_{a,i}) + \tau_b \cdot \eta_b + \sum_{i=1}^n (\tau_{c,i} \cdot \eta_{c,i}) \right\} \quad (5)$$

where η_a , η_b , and η_c are the area ratios for zone A, zone B, and zone C on the shear failure surface.

Fig.17 compares the experimental value, $f_{s,exp}$, and the calculated value, $f_{s,cal}$, of the pile shaft resistance. In the calculation, the horizontal earth

pressure was evaluated by dividing zone A (backfilled sand) and zone C into 12 segments ($n = 12$). For $R/d = 0.75$, zones A and C overlap. Therefore, the horizontal earth pressure was evaluated assuming that zone B does not exist ($\eta_a = \eta_c = 0.5$, $\eta_b = 0$). The pile shaft resistance calculated using the proposed calculation method agrees with the experimental results in the range of -5 to +20%. In addition, this calculation method was found to be consistent with the experimental results even when applied to the conditions of the previous studies [14,15]. The evaluation of the pile shaft resistance confirmed that about six divisions of zones A and C are sufficient.

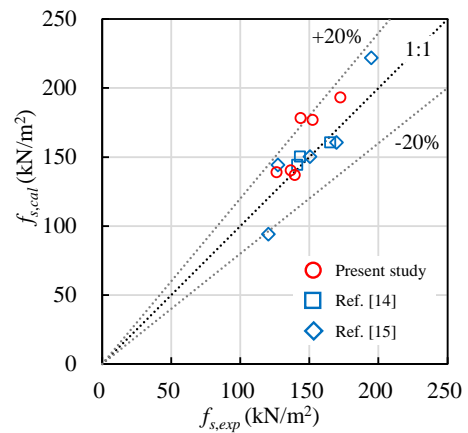


Fig.17 Comparison of experimental value, $f_{s,exp}$, and calculated value, $f_{s,cal}$, of pile shaft resistance

7. CONCLUSIONS

In this study, loading tests of a model pile overlapping backfilled sand were conducted by varying the dimensions, location, and density of the backfilled sand. The main results are summarized below.

(1) When the density of the backfilled sand is low, the maximum shaft resistance of the pile depends on the circumferential proportion of the pile in contact with the backfilled sand and the surrounding soil. When the density of the backfilled sand is high, the resistance depends on the width of the backfilled sand, which is determined by the geometrical configuration of the dimensions and location.

(2) The horizontal earth pressure at the location of shear failure near the pile, which is estimated from the measured earth pressure, varies linearly with increasing backfilled sand width. It decreases slightly for low-density backfilled sand and increases for high-density backfilled sand.

(3) A method was developed to evaluate the horizontal earth pressure at the shear failure location, which contributes to the shaft resistance of

the pile, by dividing the pile into multiple segments in the circumferential direction and performing calculations with the resulting backfill width for each segment.

(4) Introducing the evaluation of horizontal earth pressure according to the backfilled sand width led to a method for calculating the maximum shaft resistance of the pile, considering the dimensions and location of the backfilled sand. The calculated pile shaft resistance was in good agreement with the experimental results.

8. ACKNOWLEDGMENTS

The authors express their gratitude to the members of the research group at the Muroran Institute of Technology for gathering the data for this paper. This work was supported by the KAKENHI program of the Japan Society for the Promotion of Science.

9. REFERENCES

- [1] Lehane B.M. and White D.J., Lateral stress changes and shaft friction for model displacement piles in sand. *Canadian Geotechnical Journal*, Vol. 42, Issue 4, 2005, pp. 1039-1052.
- [2] Lehane B.M., Gaudin C. and Schneider J.A., Scale effects on tension capacity for rough piles buried in dense sand. *Géotechnique*, Vol. 55, Issue 10, 2005, pp. 709-719.
- [3] Loukidis D. and Salgado R., Analysis of the shaft resistance of non-displacement piles in sand. *Géotechnique*, Vol. 58, Issue 4, 2008, pp. 283-296.
- [4] Loukidis D. and Salgado R., Modeling sand response using two-surface plasticity. *Computers and Geotechnics*, Vol. 36, Issue 1-2, 2009, pp. 166-186.
- [5] Mascarucci Y., Miliziano S. and Mandolini A., A numerical approach to estimate shaft friction of bored piles in sands. *Acta Geotechnica*, Vol. 9, Issue 3, 2014, pp. 547-560.
- [6] Liu J., Zou D. and Kong X., A three-dimensional state-dependent model of soil-structure interface for monotonic and cyclic loadings. *Computers and Geotechnics*, Vol. 61, 2014, pp. 166-77.
- [7] Lashkari A., Prediction of the shaft resistance of nondisplacement piles in sand. *International Journal for Numerical and Analytical Methods in Geomechanics*, Vol. 37, Issue 8, 2013, pp. 904-931.
- [8] Lashkari A., A simple critical state interface model and its application in prediction of shaft resistance of non-displacement piles in sand. *Computers and Geotechnics*, Vol. 88, 2017, pp.95-110.
- [9] Tehrani F.S., Han F., Salgado R., Prezzi M., Tovar R.D. and Castro A.G., Effect of surface roughness on the shaft resistance of non-displacement piles embedded in sand. *Géotechnique*, Vol. 66, Issue 5, 2016, pp. 386-400.
- [10] Fakharian K. and Vafaei N., Effect of density on skin friction response of piles embedded in sand by simple shear interface tests. *Canadian Geotechnical Journal*, Vol. 58, Issue 5, 2021, pp. 619-636.
- [11] Jitsangiam P., Pra-ai S., Boulon M., Jenck O., Chen X. and Techavorasinsakul S., Characterization of a soil-rough structure interface using direct shear tests with varying cyclic amplitude and loading sequences under a large cyclic testing cycle condition. *Acta Geotechnica*, Vol. 17, Issue 5, 2022, pp. 1829-1845.
- [12] Han F., Salgado R., Prezzi M. and Lim J., Shaft and base resistance of nondisplacement piles in sand. *Computers and Geotechnics*, Vol. 83, 2017, pp. 184-97.
- [13] Wang P., Yin Z., Zhou W. and Chen W., Micro-mechanical analysis of soil-structure interface behavior under constant normal stiffness condition with DEM. *Acta Geotechnica*, Vol. 17, Issue 7, 2022, pp. 2711-2733.
- [14] Nagai H., Shaft resistance of piles close to backfilled sand columns. *International Journal of GEOMATE*, Vol. 21, Issue 84, 2021, pp. 121-128.
- [15] Nagai H. and Nakamura K., Shaft resistance mechanism for piles close to backfilled sand and its evaluation *International Journal of GEOMATE*, Vol. 23, Issue 96, 2022, pp. 84-91.
- [16] Uesugi M., Kishida H. and Tsubakihara Y., Behavior of sand particles in sand-steel friction. *Soils and Foundations*, Vol. 28, Issue 1, 1988, pp. 107-118.
- [17] Nemat-Nasser S. and Okada N., Radiographic and microscopic observation of shear bands in granular materials. *Géotechnique*, Vol. 51, Issue 9, 2001, pp. 753-765.
- [18] Yu H.S. and Houlsby G.T., Finite Cavity Expansion in Dilatant Soils: Loading Analysis. *Géotechnique*, Vol. 41, Issue 2, 1991, pp. 173-183.